Supporting information

for Laser writing of highly conductive and anti-oxidative copper structures in liquid

Xingwen Zhou[1], Wei Guo[1], Ying Zhu[1], Peng Peng[1,2]*

1. School of Mechanical Engineering and Automation, Beihang University, Beijing 100191, China

2. International Research Institute for Multidisciplinary Science, Beihang University, Beijing 100191, China

*Corresponding author: ppeng@buaa.edu.cn

Table S1. Comparison of the electrical performance of Cu structures prepared by laser processing techniques

Precursor	Substrate	Laser source	Resistivity (Ω·m)	Square resistance (Ω·sq^{-1})	Ref.
CuO NPs	Glass	Femtosecond	5.28×10^{-4}	—	1
$Cu(COOH)_2$	Glass	355nm	2.1×10^{-5}	—	2
$Cu(COOH)_2$	PI/Glass/ITO	355nm	8.46×10^{-7}	—	3
Cu NPs	PET	532nm	—	1	4
Cu NWs	Flexible film/PI	532nm	—	18	5
Cu NPs	Glass	532/800nm	3×10^{-8}	—	6
$Cu(OH)(NO_3)$	Glass/PC	—	9.6×10^{-7}	—	7
CuO NPs	Glass	1070nm	3×10^{-7}	—	8,9
Cu NPs	Glass/PEN	532	—	1	10
$Cu(NO)_3$	PC	808nm	3.4×10^{-6}	0.17	11
Cu(Ⅱ) complex (liquid)	Transparent substrate	Various	1.1×10^{-7}*	—	12
Cu(Ⅱ) complex (liquid)	Oxide glass	532nm	3×10^{-8}	—	13
Cu(Ⅱ) complex (liquid)	Glass	488nm	6×10^{-8}	—	14
Cu(Ⅱ) complex (liquid)	**PI/Glass (selective)**	**808nm**	**4×10^{-8}**	**—**	**This study**

*Calculation based on the reported conductivity.

Table S2. Comparison of the thermal stability of Cu-based structures prepared by various techniques

Precursor	Production method	Resistivity (Ωm)	Square resistance (Ωsq^{-1})	Oxidation ambience	Oxidation time	Ref.
As-synthesized Cu NPs and Ag complex	Mask Printing followed by intense pulsed light sintering (Multi-step)	3.4×10^{-8}	—	180℃	Stable for 64 h	15
As-synthesized Cu NPs, Ag salt, and Graphene nanoplatelets	Intense pulsed light sintering followed by PDMS transfer (Multi-step)	—	8.29	180℃	Stable for 4 h	16
As-synthesized Cu-Ni NPs	Spray printing followed by intense pulsed light sintering (Multi-step)	—	1.3	85℃/85% RH	Stable for 30 days	17
Cu complex and Ag complex	Mask-printing and annealing (Multi-step)	2.32×10^{-5}	—	140℃	Stable for 64 h	18
Cu NPs and Ag salt	Mask-printing and intense pulsed light sintering (Multi-step)	—	0.1	140℃	Stable for 180 min	19
Cu complex	Low-temperature curing followed by intense pulsed light sintering (Multi-step)	3.6×10^{-8}	—	85℃/85% RH	R/R_0 increase to 1.5 even over 1000 h	20
Cu NPs	Low-temperature acid-assisted laser sintering (Multi-step)	—	＜1	85℃/85% RH	Stable for 20 min	4
Cu NWs	Spray and H_2 plasma followed by hydrophobic polymers encapsulating (Multi-step)	—	17	80℃/80% RH	Stable for 1000 min	21
$Cu(NO)_3$	Laser direct writing (One-step based on dried precursor)	3.4×10^{-6}	0.17	80℃	Stable for 24 h	11
Cu(Ⅱ) complex + Tannic acid	**Laser direct writing in liquid (One-step)**	**1.1×10^{-7}**	**—**	**100℃**	**Stable for 168 h**	**This study**

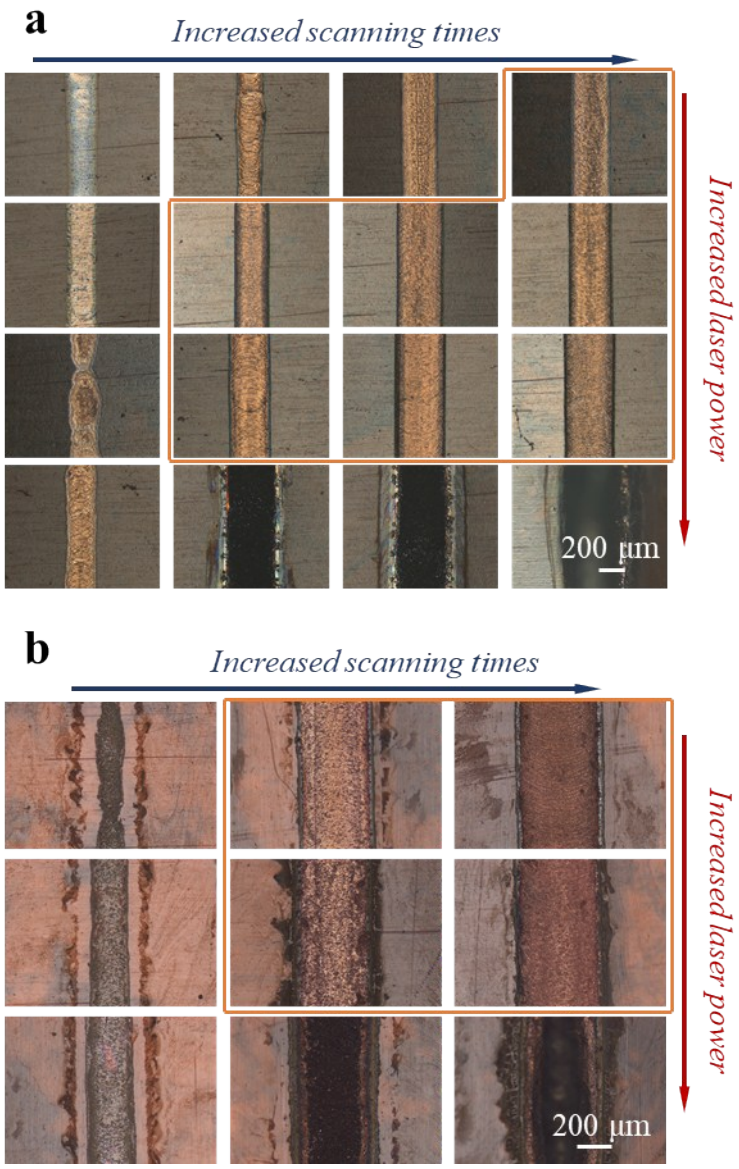

Figure S1. Surface morphologies of the (a) Cu and (b) Cu@C structures at different power density and number of scans. The process parameters correspond to the Figure 1b and Figure 1c, respectively. The small amount of C-rich accumulation would be observed surrounding the Cu@C pattern, which can be removed by a stronger detergent such as acetone.

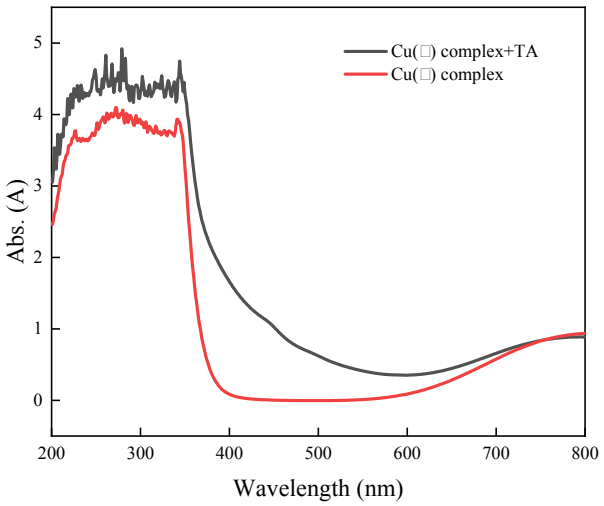

Figure S2. Absorbance of the precursors (dilute to 1%).

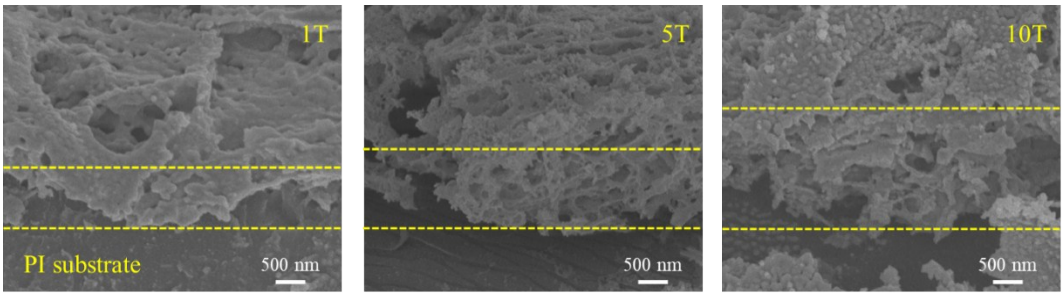

Figure S3. Tilted SEM images showing the cross-section of the Cu@C patterns as a function of the number of scans (power density = 5 W/mm^2).

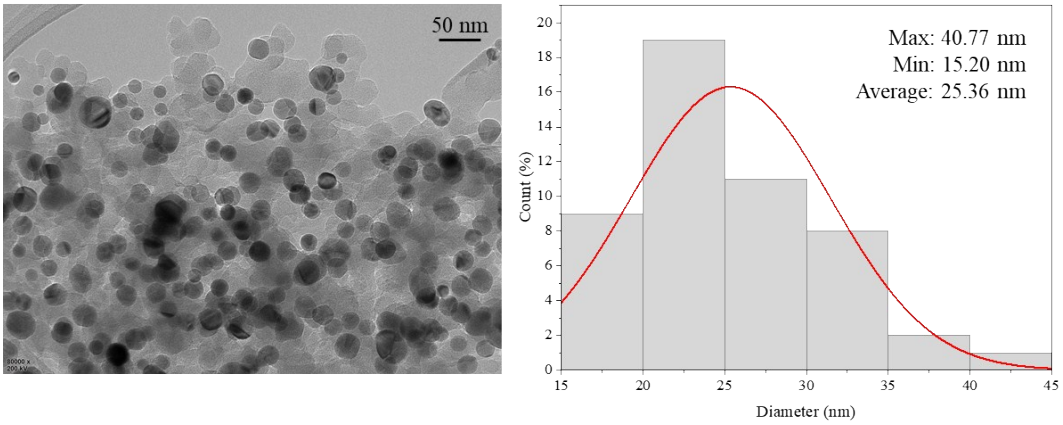

Figure S4. TEM image of a typical microstructure in Cu@C pattern with the nanoparticle size statistics (5 W·mm^2 power density at 5 scans).

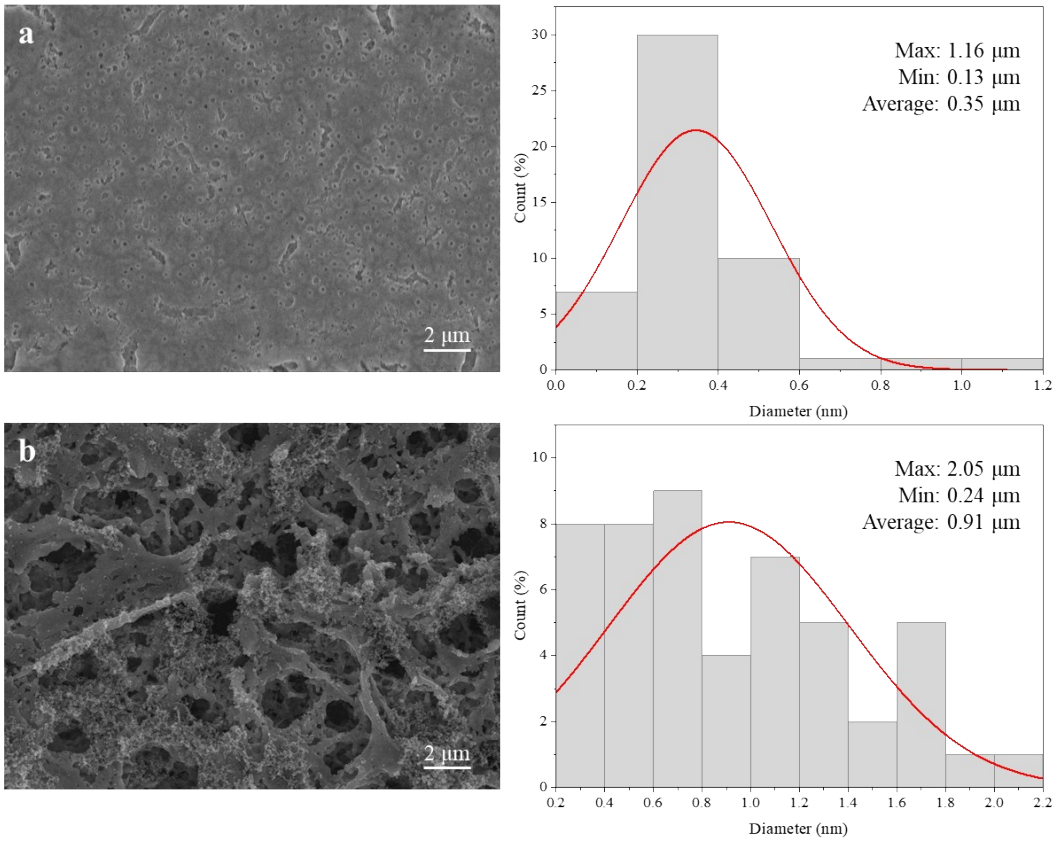

Figure S5. Comparison of the surface porosity diameter of the (a)Cu and (b)Cu@C patterns.

Table S3. Composition of the Cu@C patterns on the glass substrate as a function of scans (wt. %)

Number of scans	C	Cu	O	Na	Mg	Al	Si	Ca
1	12.36	38.13	25.62	3.77	1.02	0.27	16.27	2.56
5	12.61	45.70	19.47	3.76	0.95	—	15.10	2.42
10	13.75	81.75	3.67	—	—	—	0.42	0.4

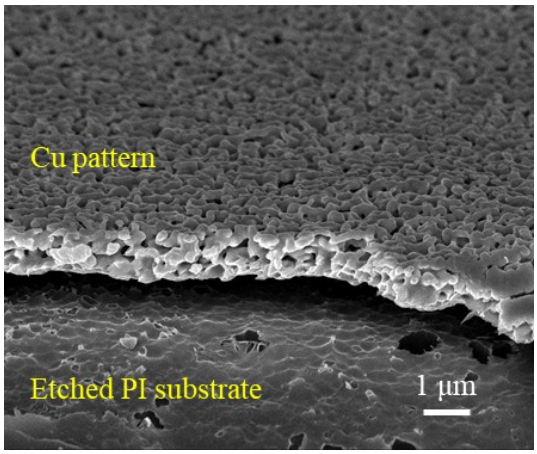

Figure S6. Tilted SEM image showing the etched PI substrate below the Cu pattern

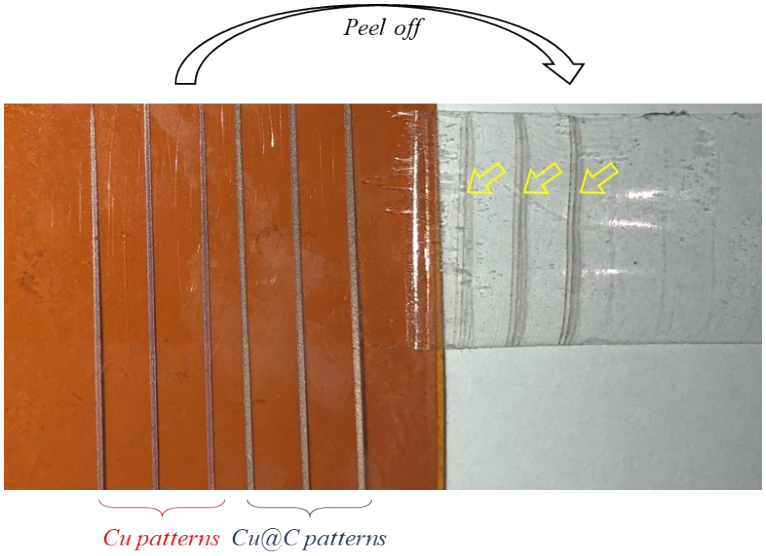

Figure S7. Digital image of the Cu and Cu@C patterns after the adhesion test. Notably, the stripped pattern attached to the tape is the C-rich accumulation in Cu@C patterns (see Figure S1). This has no significant effect on the conductivity of the Cu@C patterns.

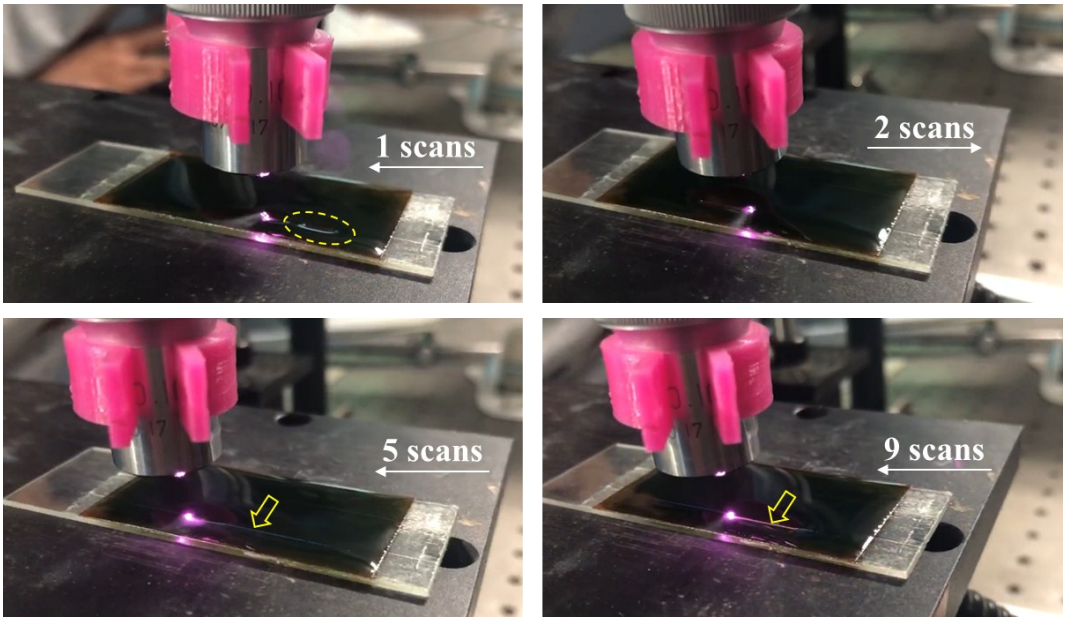

Figure S8. Observation of the *in-situ* patterning process for Cu pattern. The movement of the liquid precursor is observed (as the ellipse marked) because of the laser shocking. Intermittent scanning should be performed to provide sufficient time for the natural recovery of the liquid. The fabricated pattern becomes visible after 5 scans (as the arrows marked).

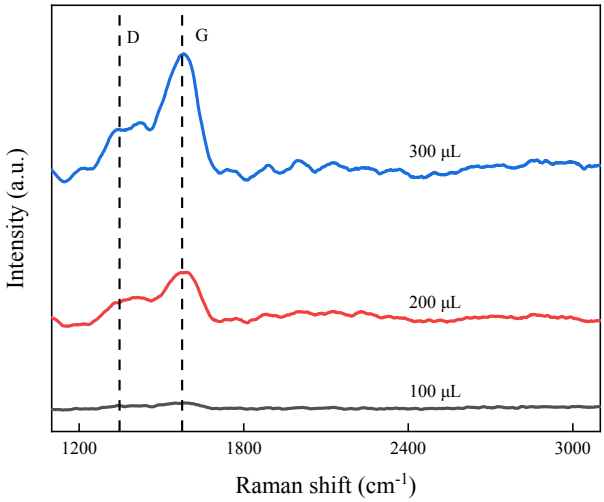

Figure S9. Raman spectra of the Cu@C pattern at various addition of tannic acid. The D-band at about 1350 cm^{-1} and G-band at about 1590 cm^{-1} are observed when the addition is higher than 200 μL, indicating the formation of graphitized or amorphous carbon [22]. Their intensities increase as the addition increases, while a further higher addition is not considered because it results in the burning of substrate during patterning.

References

1. S. Arakane, M. Mizoshiri and S. Hata, *Japanese Journal of Applied Physics*, 2015, **54**, 06FP07.
2. K. Kwon, J. Shim, J. O. Lee, K. Choi and K. Yu, *Advanced Functional Materials*, 2015, **25**, 2222-2229.
3. H. Min, B. Lee, S. Jeong and M. Lee, *Optics & Laser Technology*, 2017, **88**, 128-133.
4. J. Kwon, H. Cho, Y. D. Suh, J. Lee, H. Lee, J. Jung, D. Kim, D. Lee, S. Hong and S. H. Ko, *Advanced Materials Technologies*, 2017, **2**, 1600222.
5. S. Han, S. Hong, J. Ham, J. Yeo, J. Lee, B. Kang, P. Lee, J. Kwon, S. S. Lee, M.-Y. Yang and S. H. Ko, *Advanced Materials*, 2014, **26**, 5808-5814.
6. M. Zenou, O. Ermak, A. Saar and Z. Kotler, *Journal of Physics D: Applied Physics*, 2014, **47**.
7. S. Bai, S. Zhang, W. Zhou, D. Ma, Y. Ma, P. Joshi and A. Hu, *Nano-Micro Letters*, 2017, **9**.
8. B. Kang, S. Han, J. Kim, S. Ko and M. Yang, *The Journal of Physical Chemistry C*, 2011, **115**, 23664-23670.
9. S. Back and B. Kang, *Optics and Lasers in Engineering*, 2018, **101**, 78-84.
10. J. Kwon, H. Cho, H. Eom, H. Lee, Y. D. Suh, H. Moon, J. Shin, S. Hong and S. H. Ko, *ACS Appl Mater Interfaces*, 2016, **8**, 11575-11582.
11. P. Peng, L. Li, P. He, Y. Zhu, J. Fu, Y. Huang and W. Guo, *Nanotechnology*, 2019, **30**, 185301.
12. U. Klotzbach, K. Washio, C. B. Arnold, S. Zehnder, P. Lorenz, M. Ehrhardt, K. Zimmer and P. Schwaller, presented in part at the Laser-based Micro- and Nanoprocessing VIII, 2014.
13. V. A. Kochemirovsky, E. M. Khairullina, S. V. Safonov, L. S. Logunov, I. I. Tumkin and L. G. Menchikov, *Applied Surface Science*, 2013, **280**, 494-499.
14. V. A. Kochemirovsky, L. S. Logunov, S. V. Safonov, I. I. Tumkin, Y. S. Tver'yanovich and L. G. Menchikov, *Applied Surface Science*, 2012, **259**, 55-58.
15. W. Li, D. Hu, L. Li, C.-F. Li, J. Jiu, C. Chen, T. Ishina, T. Sugahara and K. Suganuma, *ACS Applied Materials & Interfaces*, 2017, **9**, 24711-24721.
16. C. Yim, Z. A. Kockerbeck, S. B. Jo and S. S. Park, *ACS Appl Mater Interfaces*, 2017, **9**, 37160-37165.
17. T. G. Kim, H. J. Park, K. Woo, S. Jeong, Y. Choi and S. Y. Lee, *ACS Appl Mater Interfaces*, 2018, **10**, 1059-1066.
18. W. Li, C. F. Li, F. Lang, J. Jiu, M. Ueshima, H. Wang, Z. Q. Liu and K. Suganuma, *Nanoscale*, 2018, **10**, 5254-5263.
19. C. Yim, A. Sandwell and S. S. Park, *ACS Appl Mater Interfaces*, 2016, **8**, 22369-22373.
20. W. L. Li, Y. Yang, B. W. Zhang, C. F. Li, J. T. Jiu and K. Suganuma, *Advanced Materials Interfaces*, 2018, **5**.
21. H. Zhai, R. Wang, X. Wang, Y. Cheng, L. Shi and J. Sun, *Nano Research*, 2016, **9**, 3924-3936.
22. J. Cai, C. Lv and A. Watanabe, *Nano Energy*, 2016, **30**, 790-800.